PHYSICAL REVIEW B **73**, 144406 (2006)

Electron correlation effects on the magnetostructural transition and magnetocaloric effect in $Gd_5Si_2Ge_2$

Durga Paudyal,[1] Vitalij K. Pecharsky,[1,2,*] Karl A. Gschneidner, Jr.,[1,2] and Bruce N. Harmon[3]
[1]*Materials and Engineering Physics Program, Ames Laboratory, Iowa State University, Ames, Iowa 50011-3020, USA*
[2]*Department of Materials Science and Engineering, Iowa State University, Ames, Iowa 50011-3200, USA*
[3]*Condensed Matter Physics Program, Ames Laboratory, Iowa State University, Ames, Iowa 50011-3020, USA*

(Received 26 January 2006; revised manuscript received 28 February 2006; published 6 April 2006)

Electron correlation effects on the electronic structure of $Gd_5Si_2Ge_2$ have been studied using the tight binding linear muffin-tin orbital method within the framework of the local spin density approximation with the Coulomb correlation parameter approach. The magnetostructural transition temperature (T_M) and the magnetocaloric effect (isothermal magnetic entropy change, ΔS_M) have been calculated using this method by applying the scalar relativistic band theory and the nonlocal exchange correlation parametrization of the exchange correlation potential together with a magnetothermodynamic model. Both T_M and ΔS_M are in good agreement with experimental values.

DOI: 10.1103/PhysRevB.73.144406 PACS number(s): 61.10.−i, 61.50.Ks, 71.20.−b

I. INTRODUCTION

Numerous experimental studies indicate that $Gd_5Si_2Ge_2$ undergoes a magnetostructural transformation around room temperature and exhibits unusually large magnetoresistance, magnetostriction and magnetocaloric effects.[1] The latter phenomenon makes this compound a promising material to use for near room temperature magnetic refrigeration applications. A martensiticlike, displacive structural transition from an orthorhombic to a monoclinic phase occurs simultaneously with the ferromagnetic to paramagnetic transition on heating, and the reverse transformations are observed on cooling with the magnetic and structural transitions remaining fully coupled. Below room temperature, therefore, $Gd_5Si_2Ge_2$ adopts the orthorhombic ferromagnetic state and around room temperature it exists in a monoclinic paramagnetic phase. In addition to temperature, the same magnetostructural transition is easily triggered by magnetic field and hydrostatic pressure when either is applied above the zero field, ambient pressure transformation temperature.

Crystallography and basic magnetic properties of several $Gd_5Si_xGe_{4-x}$ compounds have been reported first by Smith *et al.*[2] and Holtzberg *et al.*[3] in 1967. However, these materials did not receive much attention until 1997 when Pecharsky and Gschneidner[4] discovered the giant magnetocaloric effect in $Gd_5Si_2Ge_2$. The largest near room temperature magnetocaloric effect observed previously in the elemental gadolinium was nearly doubled. Following this discovery, $Gd_5Si_xGe_{4-x}$ and related $R_5Si_xGe_{4-x}$ materials have enjoyed a broad interest.[5–21] Physical fundamentals governing their potent magnetocaloric effect and other magnetoresponsive effects, such as the giant magnetoresistance and the colossal magnetostriction were discovered[5,6] soon after the giant magnetocaloric effect was reported.

The physics of the $Gd_5Si_xGe_{4-x}$ system is intimately related to the peculiar crystal structures of its members in which Gd, Si, and Ge atoms are arranged into two-dimensional nanolayers (slabs) whose spatial arrangement (a total of 36 atoms per unit cell) is determined by a number of covalentlike Si/Ge-Si/Ge bonds between the neighboring slabs (0, 2 or 4 covalently bonded pairs of atoms per unit cell). A change in the number of the interslab Si_2 (Ge_2 or SiGe) pairs drastically modifies the crystallography,[22,23] electronic structure,[24] and magnetic interactions[25,26] in the system. Whereas the intralayer magnetic interactions can be described by the Rudermann-Kittel-Kasuya-Yosida (RKKY) indirect $4f$-$4f$ exchange, commonly accepted as the main mechanism for magnetic interactions in $4f$ intermetallics, the formation of covalentlike interslab bonds is believed to be capable of enhancing the interlayer coupling by means of a superexchange type interaction mediated via a network of Gd-Si/Ge-Si/Ge-Gd bonds connecting the slabs, thus allowing the existence of different magnetic states.[1,27] As a matter of fact, a coupled magnetostructural phase transition occurs in $Gd_5Si_2Ge_2$ on heating to around 270 K. The high temperature paramagnetic phase adopts the monoclinic structure with two interslab bonds per unit cell and the low temperature ferromagnetic phase realizes the orthorhombic structure with all four of the Si/Ge-Si/Ge pairs per cell formed.[1] The coexistence of the crystallographic transformation with the ferromagnetic ordering gives rise to an additional source of the magnetic field-induced isothermal entropy change, consequently providing the explanation of the giant magnetocaloric effect.[28] Thus, this magnetostructural transformation that can be reversibly induced by changing temperature, magnetic field and/or pressure is at the origin of rich and complex phenomenology that has been described in the past.[3–6,9–32]

In this study, our aim is to understand electronic and magnetic properties of gadolinium alloyed with silicon and germanium from first principles electronic structure theory and then use the outputs, e.g., exchange coupling energies and magnetic moments, to compute finite temperature properties, namely magnetization, magnetic entropy, magnetostructural transition temperature and, ultimately, the magnetocaloric effect through thermomagnetic models. To date, there is no well tested, realistic approach to estimate the magnetocaloric effect using parameters calculated from first principle electronic structure theory, and therefore, our aim here is also to test some approaches, leading to calculation of the magnetocaloric effect in the $Gd_5Si_2Ge_2$ system.

An early first principles study of this system using the local spin density approximation, LSDA,[24] led to an estimated magnetostructural transition temperature (T_M) of 61 K, i.e., much smaller than the 276 K observed experimentally. A more recent study with traditional multiple scattering using the LSDA+U approach improves the estimated T_M to 206 K.[33] On the other hand, many of the magnetic properties of elemental gadolinium are well understood, and many experimental observations are closely reproduced using the LSDA+U approach.[34,35] Indeed, this should also be true for the $Gd_5Si_2Ge_2$ and related $Gd_5Si_xGe_{4-x}$ compounds. A study of[36] $Gd_5Si_2Ge_2$ using mean field model with model parameters chosen to fit experimental values indicates that first order ferromagnetic-paramagnetic phase transition influences the magnetocaloric effect via combined effects of magnetic field, pressure, and magnetoelastic deformation. Nóbrega *et al.*[37] examine magnetocaloric effect using classical Monte Carlo simulations for second-order materials $Gd_5Si_{3.2}Ge_{0.8}$ and Gd_5Si_4 opening up a possibility to calculate the magnetocaloric effect in first order materials such as $Gd_5Si_2Ge_2$. Since these phenomenological studies with adjustable parameters provide theoretical estimates of the magnetocaloric effect, coupling of electronic structure with these models should provide further microscopic insights leading to a better understanding of the magnetostructural transition and the magnetocaloric effect in these materials. We begin with a systematic study of the $Gd_5Si_2Ge_2$ system (probably the best studied composition to date) using both local and nonlocal exchange correlation functionals in the electronic structure theory within the LSDA+U approach[38] and using the tight binding linear muffin tin orbital (TB-LMTO) method[39] focusing on the role of both electron correlation and exchange correlation functionals in the electronic structure for the accurate determination of physical quantities.

Here, we calculate the total energies and compute energies of formation in both the monoclinic and orthorhombic phases to study the relative stability of this compound in these two structures. We calculate the magnetic moments of gadolinium atoms in both polymorphic modifications of $Gd_5Si_2Ge_2$ considering ferromagnetic and antiferromagnetic arrangements of spins. The magnetic structures are described in terms of exchange coupling between the nearest neighbor local moments. There is a competition between electronic potential energy, which favors ordered magnetism, and the electronic kinetic energy, which favors a paramagnetic (disordered) spin structure. Finally, we calculate the exchange coupling energy as the difference in total energies of the ferromagnetic and antiferromagnetic types of atomic spin configuration. Using these computed exchange interaction energies, we have applied the Heisenberg model to deduce the Curie temperature. We then compute the magnetostructural transition temperature and the magnetocaloric effect using magnetothermodynamic models[40] with parameters obtained from first principle calculations.

II. EXPERIMENTAL INFORMATION: CRYSTAL AND MAGNETIC STRUCTURES

From x-ray powder and single crystal diffraction experiments,[22,23] it is well established that $Gd_5Si_2Ge_2$ has an orthorhombic (space group *Pnma*) Gd_5Si_4-type crystal structure at low temperature. Around room temperature, it transforms into a monoclinic (space group $P112_1/a$) $Gd_5Si_2Ge_2$-type crystal structure via a martensiticlike distortion from the Gd_5Si_4-type orthorhombic *Pnma* structure. In the monoclinic structure, the angle between the **a** and **b** basis vectors is no longer 90°, and both the mirror plane *m* perpendicular to **b** and the glide plane *n* perpendicular to **a** vanish. However, the glide plane, *a*, which is perpendicular to **c**, the screw axis 2_1 parallel to **c**, and the center of inversion remain unaffected by this distortion. The resulting space group symmetry, $P112_1/a$, is a subgroup of *Pnma*. Atoms located in the general site of the space group *Pnma* (the multiplicity of these sites is 8) break into two symmetrically independent sets of atoms located in two general fourfold sites in the monoclinic symmetry. Furthermore, atoms in special sites, i.e., those that are located on the mirror planes in the orthorhombic crystal system, where the value of the *y* coordinate has been fixed at $y=\frac{1}{4}$, are no longer special sites and their *y* coordinates become free parameters.

The two polymorphs of $Gd_5Si_2Ge_2$ that are shown in Fig. 1 are conveniently described in terms of nearly two-dimensional, ~7 Å-thick slabs formed by strongly bonded Gd, Si, and Ge atoms. The slabs interact with one another via the *T*1 sites occupied by Si (around 40%) and Ge (around 60%). At low temperature, these latter Si and Ge atoms form stronger bonds, due to a smaller interatomic separation, connecting the slabs together, thus enhancing interslab interactions. In this case, the bonding between all slabs is identical. Because of this nearest neighbor and next nearest neighbor slab bonding changes, there occurs a ferromagnetic alignment of intra (via RKKY type indirect 4*f*-4*f* exchange) as well as inter slab Gd atoms (presumably by means of superexchange type interaction mediated via Gd-Si/Ge-Ge/Si-Gd bonds). When the temperature is increased to about room temperature, there occurs a shear displacement of the pairs of slabs and the (Si-Ge) and (Ge-Si) bonds that connected every other slab become long (bond distances are increasing from ~2.6 to 3.5 Å), and therefore, the crystal structure no longer remains orthorhombic but transforms to the monoclinic structure. With the movement of the pairs of slabs, the new structure is no longer ferromagnetic, but transforms to a paramagnet. This process is fully reversible, i.e., when the temperature is reduced $Gd_5Si_2Ge_2$ again orders ferromagnetically simultaneously with a crystallographic change to the orthorhombic phase, during which the slabs reverse the movements with respect to one another in a shear fashion and all interslab Si/Ge-Si/Ge bonds reappear. There is a noticeable hysteresis involved with this transformation.

III. ELECTRONIC STRUCTURE

The LSDA+U correlated band approach[34] has been employed to investigate the electronic and magnetic properties

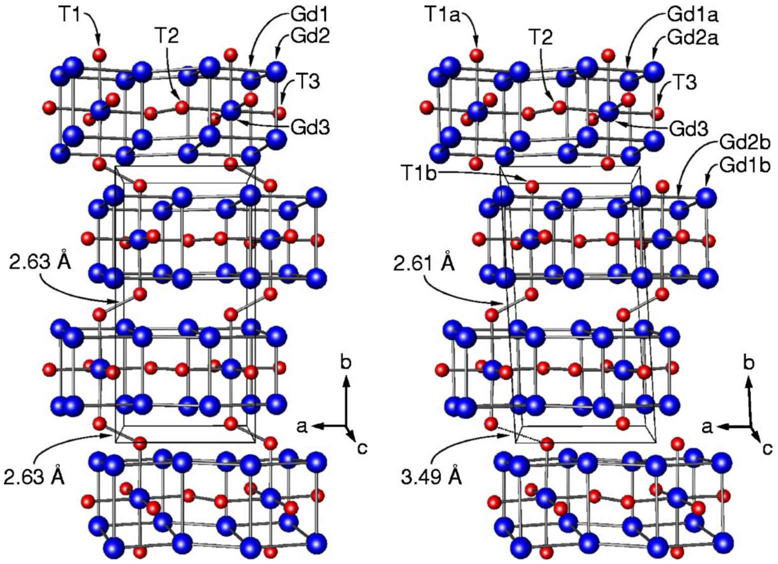

FIG. 1. (Color online) The crystal structures of the orthorhombic (left) and monoclinic (right) phases of $Gd_5Si_2Ge_2$. $T1$ in the orthorhombic and $T1a$, $T1b$ in the monoclinic structures represent the Si/Ge atoms in the interslab positions, henceforth referred as T' sites, and $T2$, $T3$ in both phases represent the Si/Ge atoms in intraslab positions (henceforth the T sites).[23] Numerical values highlight interslab Si/Ge-Si/Ge bond lengths together with the most considerable changes in the interslab T'-T' distances. Intraslab distances change insignificantly, i.e., they differ by less than 5% in the two polymorphs.[23]

of the $Gd_5Si_2Ge_2$ system. Using LSDA+U, the localized $4f$ electrons of gadolinium atoms in this system can be suitably treated. The LSDA+U method starts from the LSDA total energy, which is supplemented by an additional intra-atomic Coulomb correlation term (U) and exchange interaction term (J) of multiband Hubbard type minus a so-called double counting term to subtract the electron-electron interactions already included in LSDA. Our calculations are performed using the scalar relativistic version (which includes the mass velocity and Darwin correction terms)[41] of the LSDA+U method implemented in the tight binding linear muffin tin orbital (TB-LMTO) within the atomic sphere approximation[39] with $U=6.7$ eV and $J=0.7$ eV.[38] In our calculations, first we have adopted the conventional von Barth and Hedin[42] parametrization of the LSDA which is well known as one of the local exchange correlation functionals and, later, we have also used the Langreth, Mehl, and Hu[43] parametrization, known as a nonlocal exchange correlation functionals. Furthermore we have used 125 and 170 special k points in the irreducible part of the Brillouin zone for k space integration in the orthorhombic and monoclinic phases, respectively.

Experimentally determined[23] atomic parameters in $Gd_5Si_2Ge_2$ show that the Ge and Si atoms in the inter-slab (T') and intraslab (T) positions are populated slightly differently. Thus, the T' sites are occupied by 60% Ge and 40% Si atoms and the T sites are occupied by 40% Ge and 60% Si atoms. For theoretical calculations, we put Ge atoms in the T' and Si in the (T) positions as a first model and then Si in (T') and Ge atoms in (T) positions as a second model. Then we take statistical averages of the outputs like total energy and magnetic moments obtained with these models according to the experimentally determined occupancies of the interslab and intraslab sites by Ge and Si atoms.

IV. RESULTS AND DISCUSSIONS

In Fig. 2, the change in the total energy as a function of angle β in the monoclinic phase is shown, assuming the ferromagnetic ordering of Gd atoms for the electronic structure calculations. There is a slight increase in the total energy from 90° to 93° and then it remains nearly constant between 93° and 96°. The experimentally determined monoclinic angle in $Gd_5Si_2Ge_2$ is 93.26°. For comparison, the calculated total energy of the ferromagnetic orthorhombic structure is compared with the values obtained for the monoclinic phase. In all cases the total energies are slightly lower when T' positions are occupied by Ge atoms and T positions by Si compared to the T' positions occupied by Si and T positions by Ge. The difference in the total energies of the the monoclinic and orthorhombic phases is ~8 mRyd/atom, indicating that the orthorhombic ferromagnetic phase is the ground state structure with lower energy. The monoclinic phase with $\beta=90°$ differs by ~6 mRyd/atom from the orthorhombic phase. The monoclinic phase with $\beta=90°$ and experimentally determined stable monoclinic phase with $\beta=93.26°$ differ by ~2 mRyd/atom. These results indicate that the change in the total energy between the orthorhombic and the monoclinic phases is mainly due to the rearrangement in stacking of the slabs along the b axis.

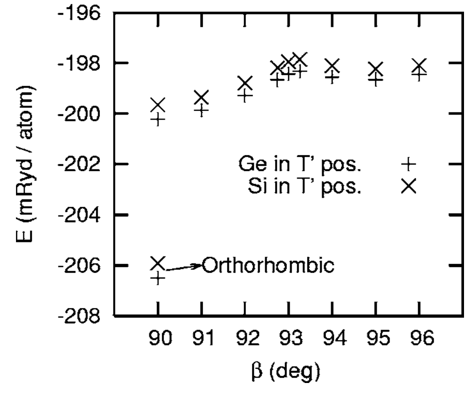

FIG. 2. Variation of the total energy as a function of angle β in the monoclinic $Gd_5Si_2Ge_2$ phase. The total energy of the orthorhombic phase is compared at $\beta=90°$. The zero of the total energy is taken as −13 577 Ryd/atom. All calculations are for ferromagnetic ordering.

A. Energy of formation

The energies of formation of the $Gd_5Si_2Ge_2$ alloy have been computed from the total energies of the alloy and the components in both the monoclinic and orthorhombic phases to probe the relative stability of these two phases. The energy of formation, E_f, of a three component alloy system can be written as

$$E_f = E_t(V_t) - c_A E_A(V_A) - c_B E_B(V_B) - c_C E_C(V_C), \quad (1)$$

where V_t, V_A, V_B, and V_C are volumes of the alloy and components, respectively, c_A, c_B, and c_C are atomic fractions of the components of the alloy and E_t, E_A, E_B, and E_C are the total energies of the alloy and components, respectively. Using this relation, computed energies of formation of both the orthorhombic and monoclinic $Gd_5Si_2Ge_2$ phases are negative. The energy of formation of the orthorhombic phase is lower (−98.48 mRyd/atom) than that of the monoclinic phase (−90.35 mRyd/atom). In Table I, the total valence charges (number of electrons) in different atomic spheres in the orthorhombic and monoclinic phases are shown. Ideally (assuming no charge transfer), there should be ten electrons beyond the Xe core ($4f^7 5d^1 6s^2$) in gadolinium and four in each germanium ($4s^2 4p^2$) and silicon ($3s^2 3p^2$) atoms beyond their respective noble gas cores, Ar and Ne. Our calculations show that in the orthorhombic phase, the total electronic charges in some of the gadolinium atoms (Gd1 and Gd3) are only slightly higher than ten (seven electrons out of ten are $4f$ electrons which are localized and do not take part in charge transfer, only $5d$ and $6s$ electrons do) and in germanium and silicon they are slightly lower than four. Therefore, the charge transfer effect in the orthorhombic phase is minimal and, consequently, the Madelung energy is close to zero. But in the monoclinic case we find that the electronic charges of some of the gadolinium atoms (specifically, Gd1*a* and Gd2*a*) are considerably larger than ten and some of the germanium and silicon atoms are notably lower than four. Thus the atomic spheres in the monoclinic phase are no longer charge neutral. It is worth to point out here that the sphere radii used in this calculation have been determined considering the corresponding experimental lattice parameters of the orthorhombic and monoclinic $Gd_5Si_2Ge_2$ structures. The importance of these radii for the site projected magnetic moments of Gd in $Gd_5Si_2Ge_2$ is pointed out in the following section. The difference in the formation energies of the two phases is the energy which transforms the lower symmetry monoclinic phase to the higher symmetry orthorhombic phase. Experimentally it has been found that the monoclinic paramagnetic phase is stable in the temperature range from ~276 K to ~573 K.[23,44] It is quite unusual for the low temperature phase of a material to have higher symmetry than the high temperature phase. There is in this case the issue of magnetism, i.e., magnetic exchange coupling energy at finite temperature that plays a crucial role in determining the stability of the ferromagnetic orthorhombic phase compared to that of the monoclinic magnetically disordered polymorph. As pointed out in the Introduction, in the low temperature ferromagnetic orthorhombic phase, in addition to the RKKY exchange, there may exist a direct Gd-T'-T'-Gd superexchange propagating through the interlayer covalentlike bonds. The bond breaking between the slabs which occurs at the structural transformation leads to the disappearance of the superexchange interaction, the long range ferromagnetism is abruptly destroyed and the material becomes paramagnetic. Therefore the magnetic exchange coupling energy is higher in the ferromagnetic orthorhombic phase due to the RKKY and superexchange mechanisms compared to the monoclinic phase (which is discussed in Sec. C, below). Indeed, there is a high temperature $Gd_5Si_2Ge_2$ phase where the monoclinic structure transforms into another orthorhombic paramagnetic phase,[44] i.e., the conventional symmetry rela-

TABLE I. Total charges (Q) [$6s$, $6p$, $5d$, and $4f$ for Gd and $3(4)s$ and $3(4)p$ for Si(Ge)] obtained from self-consistent electronic structure LSDA+U calculation employing specified atomic radii (R in au.). O and M represent orthorhombic and monoclinic phases, respectively.

	R	Q
	O Ge in T' positions and Si in T positions	
Gd1	3.72	10.06
Gd2	3.56	10.00
Gd3	3.63	10.08
Ge1	3.01	3.96
Si2	2.96	3.95
Si3	2.96	3.93
	O Si in T' positions and Ge in T positions	
Gd1	3.72	10.06
Gd2	3.56	10.00
Gd3	3.63	10.09
Si1	3.01	3.98
Ge2	2.96	3.92
Ge3	2.96	3.90
	M Ge in T' positions and Si in T positions	
Gd1a	3.96	10.48
Gd1b	3.52	9.88
Gd2a	3.72	10.25
Gd2b	3.43	9.76
Gd3	3.69	10.06
Ge1a	2.94	3.73
Ge1b	3.01	4.09
Si2	2.95	3.94
Si3	2.95	3.81
	M Si in T' positions and Ge in T positions	
Gd1a	3.96	10.48
Gd1b	3.52	9.88
Gd2a	3.72	10.25
Gd2b	3.43	9.77
Gd3	3.69	10.07
Si1a	2.94	3.76
Si1b	3.01	4.09
Ge2	2.95	3.91
Ge3	2.95	3.78

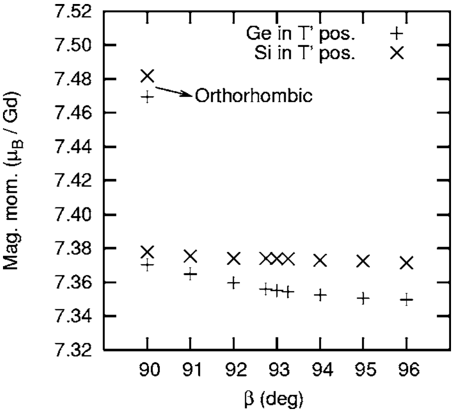

FIG. 3. Variation of average magnetic moment in Gd spheres as a function of angle β in the ferromagnetic monoclinic $Gd_5Si_2Ge_2$ phase. Average magnetic moment in Gd spheres of the ferromagnetic orthorhombic phase is compared at $\beta = 90°$.

tionships are obeyed as long as the change in the magnetic exchange energy is no longer a factor.

B. Magnetic moments

In Fig. 3, the average magnetic moment per gadolinium atom in $Gd_5Si_2Ge_2$ is shown as a function of angle β in the monoclinic phase. It should be noted that the variation in magnetic moments arise from the conduction electron and the 4f electrons remain responsible for a fixed 7 μ_B/Gd atom. The magnetic moment remains nearly constant when the interslab sites T' are occupied by Si atoms. It is also interesting to note that the magnetic moment of Gd for the Ge atoms in T' decreases with the increase of angle β until $\beta \cong 93°$ and then becomes essentially constant for $\beta > 93°$ which may indicate that preference in Ge occupations promotes the switching of the $Gd_5Si_2Ge_2$ system into the paramagnetic state in the monoclinic phase. The higher value of the average magnetic moment in the orthorhombic phase compared to that in the monoclinic phase shows that the orthorhombic phase has stronger magnetic interactions which favor it for the low temperature ferromagnetic ground state.

In Table II, magnetic moments due to outer s, p, d, and f electrons as well as total moments are shown for Gd spheres in $Gd_5Si_2Ge_2$ with ferromagnetic type of atomic spin arrangement. Magnetic moments due to f electrons are almost same and moments due to s and p electrons are negligible in each case. It is interesting to point out that the magnetic moments of 4f electrons are all slightly lower than 7.0 μ_B/Gd. It is because some $l=3$ or f character in the conduction band is negative and when we integrate for $E > E_{4f}$, the 4f magnetic moments fall slightly below 7.0 μ_B/Gd. The main differences in the magnetic moments can be seen in the d electrons of different Gd atoms in both the orthorhombic and monoclinic phases. The average magnetic moment in the orthorhombic phase is 7.47 μ_B/atom and that of monoclinic phase is 7.36 μ_B/atom, these values are slightly higher than 7.40 μ_B/atom and 7.30 μ_B/atom reported in Ref. 33. We believe this is primarily due to some differences in the theoretical and computational details. Reference 33 does not specifically point out the computational details such as sphere sizes and exchange correlation functional used in the electronic structure calculation. In our calculations, we employed the experimental lattice parameters and atomic positions from Ref. 23. The lattice parameters and atomic positions are different in the orthorhombic and monoclinic phases. Due to the differences in lattice parameters, the atomic radii are also different in the two phases. The atomic radii used in our calculations are given in Table I. The variability of the moments of different gadolinium atoms in the same phase indicates that they are not magnetically isotropic. Thus, Gd3 in the orthorhombic structure has the highest magnetic moment among the three nonequivalent gadolinium sites, and it has 6T and 8 gadolinium atoms (i.e., Gd1 and Gd2) as its nearest neighbors. The highest magnetic moment of Gd3 may be related to the shortest nearest neighbor distance between gadolinium atoms. Because of the Coulomb U parameter incorporated in the electronic structure, the 4f majority and minority band centers of gadolinium atoms are quite separated below and above the Fermi energy (the Fermi energy is −139 mRyd/atom for the orthorhombic and −151 mRyd/atom for the monoclinic phases), therefore, the majority 4f electrons which are well below the Fermi energy are localized and show localized magnetic moments. The 5d majority and minority band centers of gadolinium atoms are above the Fermi energy and these 5d electrons are the ones which play an important role in determining the magnetic properties. Interestingly, the band centers of p electrons of silicon and germanium atoms are near the Fermi

TABLE II. Spin magnetic moments (in μ_B) of different Gd atoms in $Gd_5Si_2Ge_2$. O and M represent orthorhombic and monoclinic phases respectively.

	s	p	d	f	total
	O Ge in T' positions and Si in T positions				
Gd1	0.02	0.03	0.42	6.98	7.45
Gd2	0.02	0.04	0.32	6.97	7.35
Gd3	0.02	0.06	0.53	6.97	7.59
	O Si in T' positions and Ge in T positions				
Gd1	0.02	0.04	0.43	6.97	7.46
Gd2	0.02	0.04	0.33	6.97	7.36
Gd3	0.02	0.07	0.53	6.97	7.59
	M Ge in T' positions and Si in T positions				
Gd1a	0.02	0.04	0.32	6.98	7.36
Gd1b	0.01	0.03	0.26	6.97	7.27
Gd2a	0.02	0.06	0.41	6.97	7.46
Gd2b	0.02	0.03	0.26	6.96	7.27
Gd3	0.01	0.02	0.34	6.97	7.34
	M Si in T' positions and Ge in T positions				
Gd1a	0.02	0.04	0.35	6.98	7.39
Gd1b	0.02	0.03	0.27	6.96	7.28
Gd2a	0.02	0.06	0.43	6.97	7.48
Gd2b	0.01	0.03	0.28	6.96	7.28
Gd3	0.02	0.02	0.36	6.97	7.37

TABLE III. Band centers, C (in mRyd/atom) and electron hopping parameter, Δ (in mRyd/atom) of different electronic configurations of Gd, Si, and Ge atoms in $Gd_5Si_2Ge_2$. The values in parenthesis are for minority bands. O and M represent orthorhombic and monoclinic phases, respectively. The Fermi energy for the orthorhombic phase is −139 mRyd/atom and that of the monoclinic is −151 mRyd/atom

	$\Delta_{d(p)}$	C_s	C_p	C_d	C_f
O, Ge in T' positions Si in T positions					
Gd1	48(57)	−291(−241)	454(536)	33(124)	−515(728)
Gd2	46(53)	−246(−195)	601(708)	76(164)	−479(755)
Gd3	46(56)	−272(−213)	515(613)	51(154)	−498(668)
Ge1	58(58)	−938(−937)	−122(−121)		
Si2	55(55)	−866(−862)	−125(−120)		
Si3	55(55)	−863(−861)	−120(−119)		
O, Si in T' positions and Ge in T positions					
Gd1	48(57)	−290(−240)	455(538)	34(125)	−516(710)
Gd2	46(53)	−247(−195)	599(706)	76(165)	−481(706)
Gd3	46(56)	−279(−220)	505(602)	44(147)	−507(662)
Si1	55(55)	−852(−850)	−125(−123)		
Ge2	58(58)	−955(−952)	−121(−118)		
Ge3	58(58)	−952(−951)	−117(−115)		
M, Ge in T' positions Si in T positions					
Gd1a	57(68)	−312(−273)	312(367)	20(103)	−549(831)
Gd1b	44(50)	−248(−198)	631(740)	66(150)	−494(661)
Gd2a	49(58)	−297(−246)	437(518)	33(127)	−522(672)
Gd2b	41(46)	−236(−183)	729(863)	63(149)	−491(529)
Gd3	47(55)	−300(−254)	461(540)	24(109)	−528(619)
Ge1a	57(57)	−955(−956)	−108(−108)		
Ge1b	58(58)	−942(−944)	−129(−131)		
Si2	55(55)	−884(−881)	−137(−134)		
Si3	54(54)	−864(−862)	−116(−114)		
M, Si in T' positions and Ge in T positions					
Gd1a	57(69)	−310(−270)	314(371)	22(107)	−542(857)
Gd1b	43(49)	−248(−197)	631(740)	65(150)	−497(644)
Gd2a	49(58)	−302(−251)	434(515)	29(123)	−525(685)
Gd2b	41(46)	−239(−184)	720(854)	62(149)	−493(516)
Gd3	47(55)	−299(−252)	459(539)	26(113)	−521(642)
Si1a	54(54)	−865(−864)	−113(−112)		
Si1b	55(55)	−858(−861)	−132(−135)		
Ge2	57(57)	−974(−973)	−133(−132)		
Ge3	57(57)	−953(−952)	−110(−109)		

level. The band centers of different silicon and germaniums for the orthorhombic structure are quite similar but they differ from one another in the monoclinic structure (shown in Table III). This reflects the effect of crystal symmetry in the band structure. The electron hopping parameter (Δ) for *d*-*d* electrons of gadolinium atoms differ from one another but (Δ) for *p*-*p* electrons of silicon and germanium atoms are almost identical. The dissimilarities in the band centers of the gadolinium, silicon and germanium atoms and in the electron hopping of gadolinium atoms give rise to dissimilarities in the majority and minority *d*-band electrons at the Fermi level. Figure 4 shows the spin polarized 5*d* density of states of different Gd atoms in the ferromagnetic orthorhombic structure. In both cases considering the interslab T' occupations by Ge and Si atoms, there is a clear 5*d* exchange splitting of about 50 mRyd near the Fermi level. There are dissimilarities in the 5*d* DOS (E_F) of the nonequivalent Gd atoms with Gd3 having the largest 5*d* DOS (E_F), which results in the largest magnetic moment among all three nonequivalent Gd atoms in the orthorhombic structure.

Figure 5 shows the values of the local magnetic moments of gadolinium atoms in the orthorhombic and monoclinic $Gd_5Si_2Ge_2$ phases in both $\uparrow\uparrow$ ferromagnetic (FM) type and $\uparrow\downarrow$ antiferromagnetic (AFM) type spin arrangements. The FM/AFM spin arrangement means the neighboring Gd atomic spin is aligned in parallel/antiparallel manner within

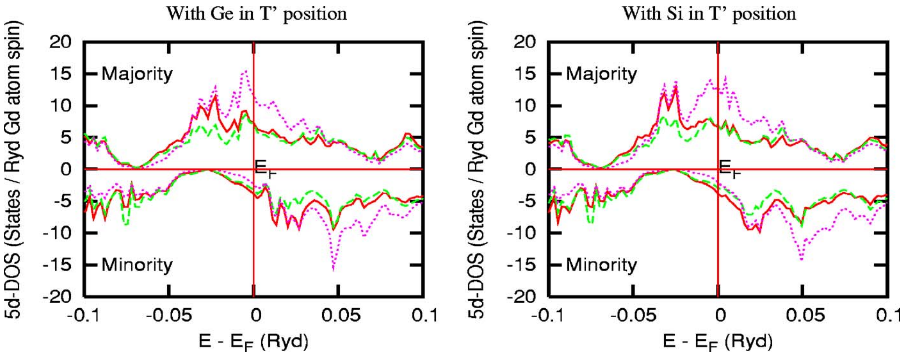

FIG. 4. (Color online) The spin polarized $5d$ density of states (DOS) of different Gd atoms in the ferromagnetic orthorhombic $Gd_5Si_2Ge_2$ phase. Solid, dashed, and dotted lines denote the corresponding $5d$ DOS of Gd1, Gd2, and Gd3 sites.

as well as between the slabs. The difference in the magnetic moments between FM and AFM spin arrangements in the orthorhombic phase is the smallest for Gd1 with Gd2 being slightly larger than Gd3. Similarly, the differences in the magnetic moment between FM and AFM spin arrangement in the monoclinic phase are the lowest in Gd1*a* and Gd3 compared to other Gd sites with Gd1*b* and Gd2*a* slightly higher than Gd2*b*. The difference in the magnetic moments between the FM and AFM states in the orthorhombic phase is greater than that in the monoclinic phase which is indicative of the higher magnetic coupling energy (discussed below) for the orthorhombic phase.

C. Magnetic exchange coupling energy and Curie temperature

Since $4f$ magnetic moments are localized, the use of Heisenberg-type Hamiltonian for the dependence of energy on spin configuration may be justified for gadolinium and its compounds assuming RKKY type exchange interactions. The spin Hamiltonian with zero external magnetic field is then given by[35]

$$H = -\sum_i \sum_\delta J_{i,i+\delta}\hat{S}_i\hat{S}_{i+\delta}, \tag{2}$$

where $J_{i,i+\delta}$ is an exchange coupling constant (J) between the spin $\hat{S}_i$ and its nearest neighbor spin $\hat{S}_{i+\delta}$ separated by δ. Then, the Curie temperature of a conventional three dimensional Heisenberg ferromagnet in the mean field approximation is given by[45]

$$T_C = ZJ\frac{S(S+1)}{3k_B} = \frac{2}{3}\frac{E_{\uparrow\downarrow} - E_{\uparrow\uparrow}}{k_B} = \frac{2}{3}\frac{J_0}{k_B}, \tag{3}$$

where, Z is the number of nearest neighbors, S is the spin momentum (the angular momentum, $L=0$ for Gd based systems), and k_B is Boltzmann's constant. J_0 is the exchange coupling energy, i.e., the difference of total energies in antiferromagnetic (↑↓) and ferromagnetic (↑↑) type spin configurations. Since simple ↑↓ and ↑↑ spin configurations of Gd atoms do not account for potentially peculiar microscopic magnetic structures of $Gd_5Si_2Ge_2$,[46,47] J_0 involves both interslab and intraslab exchange coupling contributions between the Gd-Gd neighbors. Using this relation [Eq. (3)], the calculated Curie temperatures are 260 K for the orthorhombic and 167 K for the monoclinic phases, taking occupations by Ge and Si positions in accordance with experiment.[23] The values of Curie temperatures (which can be seen from Fig. 6) with full occupations of Ge and Si in the T' positions[23] differ considerably in the monoclinic phase indicating the tendency towards ferromagnetism when T' positions are occupied by Si atoms and T positions are occupied by Ge atoms. This tendency of Si to enhance magnetic interactions while occupying the T' sites is opposite to what is observed experimen-

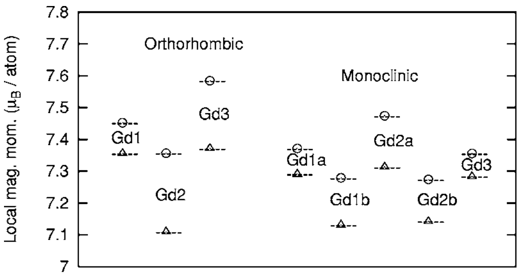

FIG. 5. The local magnetic moments of Gd atoms in the orthorhombic and monoclinic phases of $Gd_5Si_2Ge_2$ calculated using local exchange correlation functional within the LSDA+U method. The circles denote the magnetic moment with ↑↑ (FM) type atomic spin arrangement and the triangles the magnetic moment with ↑↓ (AFM) type atomic spin arrangement.

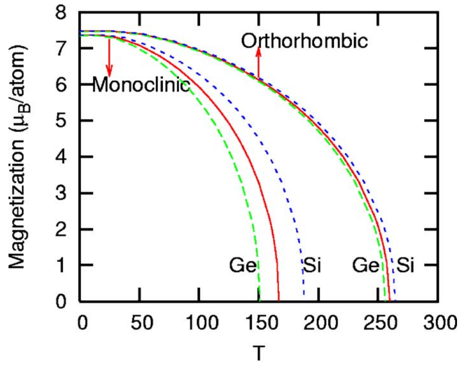

FIG. 6. (Color online) Magnetization of $Gd_5Si_2Ge_2$ as a function of temperature derived using computed saturated magnetic moments and Curie temperatures of the monoclinic and orthorhombic phases with local exchange correlation functional in the electronic structure LSDA+U calculation. The broken lines denote the magnetization with Ge atoms in (T') and Si in (T) positions and dashed lines with Si in (T') and Ge atoms in (T) positions. Solid lines denote the magnetization considering the experimental occupations of Ge and Si atoms in T' and T positions (i.e., ~60% for Ge and ~40% for Si occupations in T' and opposite in T positions).

tally and is expected from size consideration of the Si and Ge atoms which predicts that the Ge atoms occupy the T' sites. It is probably this competition between the lattice energy and the magnetic energy which accounts for the 60% occupation of the T' sites by Ge atoms.

D. Magnetization

Experimental magnetization and magnetic susceptibility data of $Gd_5Si_2Ge_2$ measured on cooling and heating exhibit hysteresis, which is typical for a first order phase transition.[27] To date, direct first principles computation of magnetization or susceptibility through a first order phase transition is not feasible. Yet, one can calculate the magnetization separately for each of the two phases and then compute the free energies and calculate the magnetostructural transition temperature (discussed below in Sec. E). Here, using the Curie temperatures and saturation magnetic moments of the monoclinic and orthorhombic phases, the following magnetization relation (Brillouin function) is solved self-consistently and the magnetization curves are obtained as shown in Fig. 6

$$\sigma = \frac{M}{M_S} = \tanh\left[\frac{3S}{S+1}\frac{M}{M_S}\frac{T_C}{T}\right]. \tag{4}$$

In the orthorhombic phase, the magnetization curves are quite similar, regardless of which atoms (Si or Ge) are placed in the interslab positions. But in the monoclinic phase, the magnetization curve is shifted to higher temperature when the Ge atoms in the interslab position are replaced by Si. This indicates that the occupation of the interslab sites by Si atoms in the monoclinic phase enhances the ferromagnetic behavior thus forcing the system to transform towards the ferromagnetic Gd_5Si_4 type phase. It is worth noting that the magnetization of the orthorhombic phase at the Curie temperature of the monoclinic phase is already near saturation, explaining the large increase of the magnetization when $Gd_5Si_2Ge_2$ transforms from the paramagnetic monoclinic to the ferromagnetic orthorhombic phase.

E. Magnetostructural transition and the magnetocaloric effect

An important characteristic of the magnetic material is the magnetic entropy. The magnetic entropy can be changed by the variation of magnetic field or temperature. The magnetic entropy and its change are closely related to the magnetocaloric effect and are used to determine the characteristics of magnetic refrigerator materials such as refrigerant capacity.

Figure 7 shows the variation of magnetic entropies with respect to temperature in the monoclinic and orthorhombic structures assuming ferromagnetic orderings. These entropies were calculated using magnetization (σ) through the relation[40]

$$S_M \simeq R\left[\ln(2S+1) - \frac{3}{2}\left(\frac{S}{S+1}\right)\sigma^2 - \frac{9}{20}\frac{(2S+1)^4-1}{[2(S+1)]^4}\sigma^4\right], \tag{5}$$

where S is spin momentum. The magnetic entropy of the orthorhombic phase corresponding to the Curie temperature

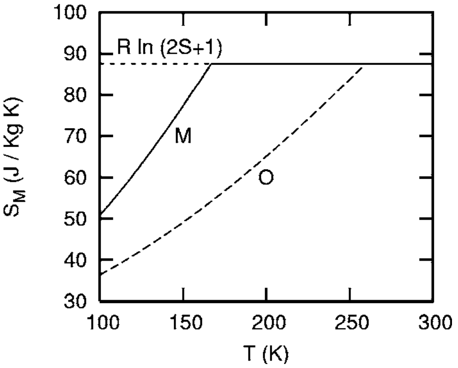

FIG. 7. Magnetic entropy as a function of temperature using magnetization obtained from saturated magnetic moment and Curie temperatures of the monoclinic and orthorhombic phases with the local exchange correlation functional used in the electronic structure LSDA+U calculation.

of the monoclinic phase is lower by $\sim 31\frac{J}{KgK}$. This indicates that the change of the magnetic entropy may be quite large when $Gd_5Si_2Ge_2$ transforms from the monoclinic to the orthorhombic phase. The computation of magnetic entropy change and its comparison with experimental results is described in the following section.

Figure 8 shows the change in magnetic free energy in both the orthorhombic and monoclinic phases calculated using magnetization and magnetic entropy through the free energy relation[40]

$$F = -\frac{3}{2}\frac{S}{S+1}RT_C\sigma^2 - TS_M. \tag{6}$$

Magnetic free energy of the monoclinic ferromagnetic phase drops off much faster with temperature than for the orthorhombic ferromagnetic $Gd_5Si_2Ge_2$ and, at 233 K the two functions become equal. This indicates the magnetic transition at T_M=233 K. Below T_M, the stable phase is ferromagnetic orthorhombic and and above this temperature it is replaced by the monoclinic phase which is already paramagnetic (see Fig. 6). Therefore the system undergoes a first order magnetostructural transition at T_M. As follows

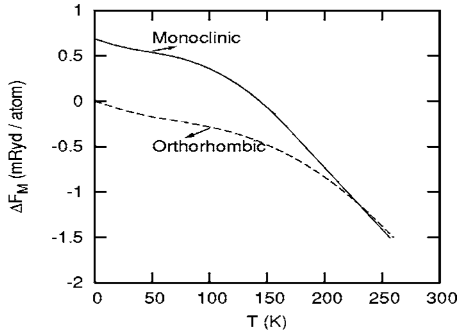

FIG. 8. Change in magnetic free energy as a function of temperature using magnetic entropy and magnetization obtained from saturated magnetic moment and Curie temperature of monoclinic and orthorhombic phases with the local exchange correlation functional used in the electronic structure LSDA+U calculation.

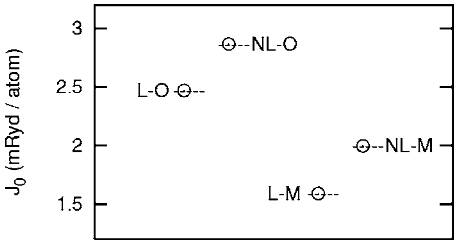

FIG. 9. Comparison of exchange coupling energies between the orthorhombic (*O*) and monoclinic (*M*) phases calculated using local (*L*) and non-local (*NL*) exchange correlation functionals within the LSDA+U method for the electronic structure.

from Fig. 6, at 233 K there is a 55% reduction in the magnetization which is close to the experimental observation (60%).[4] This transition temperature is higher than the previous value (206 K) obtained in Ref. 33 but is still somewhat lower than the experimental one (276 K on heating).

After the determination of the magnetostructural transition temperature, the magnetic entropy change can be calculated considering equal free energies at T_M

$$U_1 - T_M S_1 = U_2 - T_M S_2. \tag{7}$$

That is,

$$\Delta S = S_1 - S_2 = \frac{U_1 - U_2}{T_M}. \tag{8}$$

Here U_1 and U_2 are internal energies of the orthorhombic and monoclinic phases, respectively. Using this relation, the magnetic entropy change at the magnetostructural transition temperature is $-7.3\frac{J}{KgK}$. Thus, predicted value of the isothermal magnetic entropy change is much smaller than the experimentally observed[48] maximum entropy change of $-20\frac{J}{KgK}$. The different contributions to the entropy change are pointed out in the following section.

F. Sensitivity of the magnetostructural transition temperature and magnetocaloric effect on the exchange correlation functional

The electronic structure calculations have been repeated with the nonlocal exchange correlation functional of Langreth, Mehl, and Hu[43] within the LSDA+U in the TB-LMTO method to check whether it improves the predicted magnetostructural transition temperature. With the use of this nonlocal exchange correlation functional, there is a slight increase in the magnetic moments of the Gd atoms in the FM state and decrease in the AFM state as compared to the results obtained with the local exchange correlation functional of von Barth and Hedin.[42] Due to the change in the magnetic moments there is a significant increase of the exchange coupling energy (Fig. 9) leading to the increase of the Curie temperatures in the orthorhombic (301 K, this value is nearly identical to T_C=298 K established experimentally for the orthorhombic polymorph of $Gd_5Si_2Ge_2$)[24] and monoclinic (209 K) phases. The magnetization curves with these increased saturation magnetic moments are plotted in Fig. 10 in a manner similar to Fig. 6 but without showing separate $M(T)$ behaviors assuming different occupations of the T' sites which remain similar to those shown in Fig. 6.

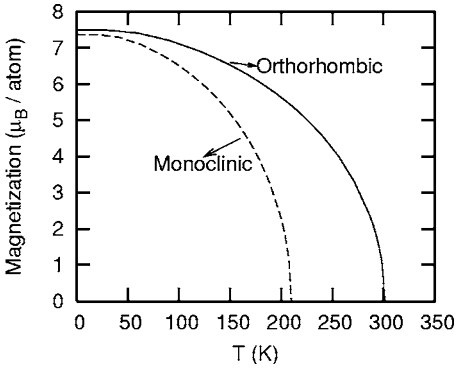

FIG. 10. Magnetization as a function of temperature using saturated magnetic moment and Curie temperature of monoclinic and orthorhombic phases with the nonlocal exchange correlation functional used in the electronic structure LSDA+U calculation.

Figure 11 shows the change in the magnetic free energy in both phases calculated using the nonlocal exchange correlation in the electronic structure calculation. The predicted magnetostructural transition temperature is 265 K. This is in nearly exact agreement with the experimental observations[24,27,48] of average T_M considering a 10 K hysteresis. Therefore, the use of nonlocal exchange correlation functional for exchange correlation potential brings a significant improvement in the magnetic transition temperature T_M compared to 233 K obtained using the local exchange correlation in the electronic structure calculation. We note that the use of the nonlocal exchange correlation functionals in Langreth, Mehl, and Hu[43] (LMH) and Perdew and Wang[49] (PW) approximations deserves some discussion. In the LMH, the gradient corrections for the correlation energy are set to zero for small values of wave vectors ($k \leq k_c$) to eliminate the unphysical contribution in the gradient expansion approximation (GEA). For the cutoff k_c, LMH uses $f\frac{\Delta n}{n}$, where n is the electron density and f is an empirical constant set to 0.15 and used for all systems. Perdew and Wang[49] on the other hand generalized the GEA by introducing cutoffs which impose sum rules in the limit of small density gradients and

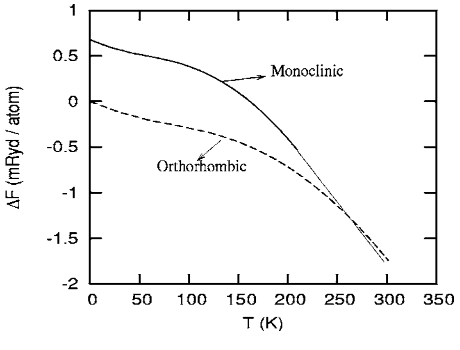

FIG. 11. Change in magnetic free energy as a function of temperature using magnetic entropy and magnetization obtained from saturated magnetic moment and Curie temperature of monoclinic and orthorhombic phases with non local exchange correlation functional in the electronic structure LSDA+U calculation.

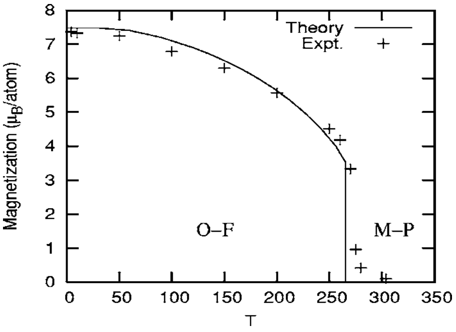

FIG. 12. Magnetization curve as a function of temperature computed using the predicted magnetostructural transition temperature from the free energy analysis of $Gd_5Si_2Ge_2$ as compared to experimentally observed values.

also contain contributions beyond the random phase approximation. The study of Bagno *et al.*[50] shows that both LMH and PW functionals eliminate the errors in the LSDA and correctly predict the ground state properties such as cohesive energy, lattice constants, and the bulk modulus of third row elements in the Periodic Table. A recent study[51] of magnetic properties of transition metal alloys, e.g., FePt, CoPt, and NiPt shows that the use of LMH functional predicts values of equilibrium lattice constants and magnetic moments which are closer to the experimental values than those obtained from the use of PW functional in the electronic structure. Our calculations on $Gd_5Si_2Ge_2$ using LSDA+U approach with von Barth and Hedin functional, discussed above, underestimates the Curie temperatures resulting in the temperature of the magnetostructural transition about 15% lower than the experimental value, while the PW functional (not discussed in this paper) overestimates the magnetostructural transition temperature by about +11%. The LMH functional resulted in an intermediate estimate for the transition temperatures, and therefore, appears to be a suitable approximation to treat the electronic structure of $Gd_5Si_2Ge_2$ and thus was adopted for the majority of the calculations.

Using thus obtained magnetostructural transition temperature using the LMH nonlocal exchange correlation functional in LSDA+U approach, the magnetization curve as a function of temperature is computed and compared with the experimentally observed spontaneous magnetic moments, extrapolated to zero magnetic field from isothermal magnetization data corresponding to different temperatures. As follows from Fig. 12, there is an excellent agreement between the theoretically calculated and experimentally observed values. The magnetization experiments were carried out by the authors of this work long ago but the spontaneous magnetization data (Fig. 12) remained unpublished.

Similarly, the isothermal magnetocaloric effect, $\Delta S_M = -8.6\frac{J}{KgK}$, calculated using nonlocal exchange correlation functional is somewhat closer to the experimentally observed value of $-20\frac{J}{KgK}$.[48] It is worth pointing out that the entropy change calculated here corresponds only to the magnetic part of the entropy change at the magnetostructural transition temperature. As follows from Ref. 52, entropy difference between the two polymorphic modification of $Gd_5Si_2Ge_2$, i.e., the contribution from the structural transformation (ΔS_{str}) into the magnetocaloric effect is $\Delta S_{str} = -9.8 \pm 0.4\frac{J}{KgK}$ at $T_M = 270$ K. Hence, the total "computed" isothermal entropy change at T_M, which can be triggered by applying magnetic field, should be $\Delta S_T = \Delta S_M + \Delta S_{str}$ resulting in $\Delta S_T = \Delta S_T^{O\text{-}F} - \Delta S_T^{M\text{-}P} = -18.4\frac{J}{KgK}$. This value establishes a discontinuity of the total entropy function of $Gd_5Si_2Ge_2$ at T_M in a zero magnetic field, noting that the magnetic part has been derived from first principles and the lattice part has been determined from experimental data. Further analysis of the experimental data from Ref. 52 in order to account for the conventional part of the magnetocaloric effect, which is dependent on the magnitude of the magnetic field change, indicates that the experimental value of the magnetic field independent discontinuity of the total entropy change of $Gd_5Si_2Ge_2$ at T_M is $\Delta S_T = -15.6 \pm 0.5\frac{J}{KgK}$. The experimental value is slightly smaller than that partly computed from first principles, which is not surprising considering that ΔS_M calculated using Eq. (8) does not account for spin fluctuations that are expected to be quite strong around $T_M = 270$ K. Furthermore, magnetostructural transition in $Gd_5Si_2Ge_2$ and related materials is magnetoelastic, and therefore, the material transforms from one state to another over a finite range of temperatures and magnetic fields, exhibiting features typical of phase separated systems, which obviously are not taken into account in our computations from first principles.

G. Effect of the magnetic field

In the presence of an external magnetic field, the free energy relation[40] is written as

$$F = -HM_S\sigma - \frac{3}{2}\frac{S}{S+1}RT_C\sigma^2 - TS_M. \tag{9}$$

The term $-HM_S\sigma$ is the interaction between the spins and the applied magnetic field. Before the application of the magnetic field the $4f$ moments of the Gd atoms are disordered and the $5d$ bands for spin up and spin down electrons are identical at the Curie temperature ($T = T_C$). If one applies an external magnetic field, it mainly aligns these $4f$ moments, which in turn spin polarizes the $5d$ electrons. This indeed gives a net $4f$ and conduction electron magnetization at the zero magnetic field Curie temperature. Due to this magnetization, the free energy functions calculated as explained in the previous section, including magnetic field, vary less sharply with temperature as compared to the zero applied magnetic field case and T_M is raised to a higher value. Our free energy analysis with an applied magnetic field shows that the magnetostructural transition temperature, $T_M = 265$ K at $H = 0$ is raised to 280 K for $H = 2$ T. Thus, the calculated value of $\frac{dT_M}{dH} = 7.5\frac{K}{T}$ is in a good agreement with the experimentally observed value of $\sim 6\frac{K}{T}$.[24]

V. CONCLUSION

By coupling the electronic structure with magnetothermodynamic models for finite temperature we have studied the magnetostructural transition and magnetocaloric effect of $Gd_5Si_2Ge_2$. This approach leads to a good agreement with already established results of the magnetostructural transition and magnetocaloric effect. Our analysis shows that the electronic structure method which takes into account strong Coulomb correlations within the framework of scalar relativistic (no spin orbit coupling) band theory works reasonably well for this system. The use a of nonlocal exchange correlation functional with the electronic structure LSDA+U method works better as compared to the local exchange correlation functional, giving a better estimate of the magnetostructural transition temperature and the magnetocaloric effect observed in $Gd_5Si_2Ge_2$. Our study shows lower value of total energy in the orthorhombic phase compared to the monoclinic phase, which confirms stability of the orthorhombic phase at low temperature. The calculated magnetic moments of the Gd atoms in this compound are larger in the orthorhombic phase than in the monoclinic phase. The variability of the magnetic moments on different Gd atoms within same phase or different phases is mostly due to the changing contribution from 5*d* electrons of Gd atoms. The magnetic exchange coupling energy of the orthorhombic phase is higher than that of the monoclinic phase.

The approach used in this work may be extended to include explicitly anisotropic magnetic coupling and form a basis for further investigations into these systems which have ferro- and antiferromagnetic correlations, respectively, within and between naturally formed slabs such as Gd_5Ge_4.

ACKNOWLEDGMENTS

This work was supported by the Office of Basic Energy Sciences, Materials Sciences Division of the U. S. Department of Energy under Contract No. W-7405-ENG-82 with Iowa State University.

---

*Corresponding author. Electronic address: vitkp@ameslab.gov

[1] V. K. Pecharsky and K. A. Gschneidner, Jr., Adv. Mater. (Weinheim) **13**, 683 (2001); and references therein.

[2] G. S. Smith, A. G. Tharp, and Q. Johnson, Acta Crystallogr. **22**, 940 (1967).

[3] F. Holtzberg, R. J. Gambino, and T. R. McGuire, J. Phys. Chem. Solids **28**, 2283 (1967).

[4] V. K. Pecharsky and K. A. Gschneidner, Jr., Phys. Rev. Lett. **78**, 4494 (1997).

[5] L. Morellon, P. A. Algarabel, M. R. Ibarra, J. Blasco, B. Garcia-Landa, J. Arnold, and F. Albertini, Phys. Rev. B **58**, R14721 (1998).

[6] L. Morellon, J. Stankiewicz, B. Garcia-Landa, P. A. Algarabel, J. Arnold, and M. R. Ibarra, Appl. Phys. Lett. **73**, 3462 (1998).

[7] N. I. Usenko, M. I. Ivanov, V. V. Berezutski, and R. I. Polotska, J. Alloys Compd. **266**, 186 (1998).

[8] A. M. Tishin and Y. I. Spichkin, *The Magnetocaloric Effect and its Applications* (Institute of Physics, Bristol, and Philadelphia, 2003).

[9] A. Giguere, M. Foldeaki, B. Ravi Gopal, R. Chahine, T.K. Bose, A. Frydman, and J. A. Barclay, Phys. Rev. Lett. **83**, 2262 (1999).

[10] J. Szade and G. Skorek, J. Magn. Magn. Mater. **196**, 699 (1999).

[11] J. R. Sun, F. X. Hu, and B. G. Shen, Phys. Rev. Lett. **85**, 4191 (2000).

[12] G. H. Rao, J. Phys.: Condens. Matter **12**, L93 (2000).

[13] F. Casanova, X. Batlle, A. Labarta, J. Marcos, L. Mańosa, and A. Planes, Phys. Rev. B **66**, 212402 (2002).

[14] J. B. Sousa, M. E. Braga, F. C. Correia, F. Carpinteiro, L. Morellon, P. A. Algarabel, and R. Ibarra, J. Appl. Phys. **91**, 4457 (2002).

[15] B. Teng, M. Tu, Y. Chen, and Jinke Tang, J. Phys.: Condens. Matter **14**, 6501 (2002).

[16] M. Nazih, A. de Visser, L. Zhang, O. Tegus, and E. Brück, Solid State Commun. **126**, 255 (2003).

[17] M. K. Chattopadhyay, M. A. Manekar, A. O. Pecharsky, V. K. Pecharsky, K. A. Gschneidner, Jr., J. Moore, G. K. Perkins, Y. V. Bugoslavsky, S. B. Roy, P. Chaddah, and L. F. Cohen, Phys. Rev. B **70**, 214421 (2004).

[18] A. M. G. Carvalho, C. S. Alves, A. de Campos, A. A. Coelho, S. Gama, F. C. G. Gandra, P. J. von Ranke, and N. A. Oliveira, J. Appl. Phys. **97**, 10M320 (2005).

[19] L. H. Lewis, M. Yu, D. O. Welch, and J. Gambino, J. Appl. Phys. **95**, 6912 (2004).

[20] A. Yan, A. Handstein, P. Kerschl, K. Nenkov, K.-H. Müller, and O. Gutfleisch, J. Appl. Phys. **95**, 7064 (2004).

[21] S. N. Ahmad, Y. Akin, and S. A. Shaheen, J. Appl. Phys. **97**, 10Q902 (2005).

[22] V. K. Pecharsky and K. A. Gschneidner, Jr., J. Alloys Compd. **260**, 98 (1997).

[23] W. Choe, V. K. Pecharsky, A. O. Pecharsky, K. A. Gschneidner, Jr., V. G. Young, Jr., and G. J. Miller, Phys. Rev. Lett. **84**, 4617 (2000).

[24] V. K. Pecharsky, G. D. Samolyuk, V. P. Antropov, A. O. Pecharsky, and K. A. Gschneidner, Jr., J. Appl. Phys. **171**, 57 (2003); G. D. Samolyuk and V. P. Antropov, J. Appl. Phys. **91**, 8540 (2002).

[25] L. Morellon, J. Blasco, P. A. Algarabel, and M. R. Ibarra, Phys. Rev. B **62**, 1022 (2000).

[26] A. O. Pecharsky, K. A. Gschneidner, Jr., V. K. Pecharsky, and C. E. Schindler, J. Alloys Compd. **338**, 126 (2002).

[27] E. M. Levin, V. K. Pecharsky, and K. A. Gschneidner, Jr., Phys. Rev. B **62**, R14625 (2000).

[28] V. K. Pecharsky, A. P. Holm, K. A. Gschneidner, Jr., and R. Rink, Phys. Rev. Lett. **91**, 197204 (2003).

[29] E. M. Levin, V. K. Pecharsky, K. A. Gschneidner, Jr., and G. J. Miller, Phys. Rev. B **64**, 235103 (2001); E. M. Levin, K. A. Gschneidner, Jr., and V. K. Pecharsky, Phys. Rev. B **65**, 214427 (2002); C. Magen, L. Morellon, P. A. Algarabel, and M. R. Ibarra, J. Phys.: Condens. Matter **15**, 2389 (2003).

[30] L. Morellon, P. A. Algarabel, C. Magen, and M. R. Ibarra, J. Magn. Magn. Mater. **237**, 119 (2001).

[31] J. Stankiewicz, L. Morellon, P. A. Algarabel, and M. R. Ibarra, Phys. Rev. B **61**, 12651 (2000).

[32] E. M. Levin, V. K. Pecharsky, and K. A. Gschneidner, Jr., Phys. Rev. B **60**, 7993 (1999); J. B. Sousa, M. E. Braga, F. C. Correia,

F. Carpinteiro, L. Morellon, P. A. Algarabel, and M. R. Ibarra, Phys. Rev. B **67**, 134416 (2003).

[33] G. D. Samolyuk and V. P. Antropov, J. Appl. Phys. **97**, 10A310 (2005).

[34] B. N. Harmon, V. P. Antropov, A. I. Lichtenstein, I. V. Solovyev, and V. I. Anisimov, J. Phys. Chem. Solids **56**, 1521 (1995).

[35] A. B. Shick, W. E. Pickett, and C. S. Fadley, Phys. Rev. B **61**, R9213 (2000).

[36] P. J. von Ranke, N. A. de Oliveira, and S. Gama, J. Magn. Magn. Mater. **277**, 78 (2004).

[37] E. P. Nóbrega, N. A. de Oliveira, P. J. von Ranke, and A. Troper, Phys. Rev. B **72**, 134426 (2005).

[38] V. I. Anisimov, F. Aryasetiawan, and A. I. Lichtenstein, J. Phys.: Condens. Matter **9**, 767 (1997).

[39] O. K. Andersen and O. Jepsen, Phys. Rev. Lett. **53**, 2571 (1984).

[40] C. P. Bean and D. S. Rodbell, Phys. Rev. **126**, 104 (1961).

[41] D. D. Koelling and B. N. Harmon, J. Phys. C **10**, 3107 (1977).

[42] U. von Barth and L. Hedin, J. Phys. C **5**, 1629 (1972).

[43] D. C. Langreth and M. J. Mehl, Phys. Rev. Lett. **47**, 446 (1981); Phys. Rev. B **28**, 1809 (1983); C. D. Hu and D. C. Langreth, Phys. Scr. **32**, 391 (1985).

[44] Y. Mozharivskyj, A. O. Pecharsky, V. K. Pecharsky, and G. J. Miller, J. Am. Chem. Soc. **127**, 317 (2005).

[45] Ph. Kurz, G. Bihlmayer, and S. Blügel, J. Phys.: Condens. Matter **14**, 6353 (2002).

[46] L. Tan, A. Kreyssig, J. W. Kim, A. I. Goldman, R. J. McQueeney, D. Wermeille, B. Sieve, T. A. Lograsso, D. L. Schlagel, S. L. Budko, V. K. Pecharsky, K. A. Gschneidner Jr., Phys. Rev. B **71**, 214408 (2005).

[47] C. Magen, L. Morellon, P. A. Algarabel, M. R. Ibarra, Z. Arnold, J. Kamarad, T. A. Lograsso, D. L. Schlagel, V. K. Pecharsky, A. O. Tsokal, and K. A. Gschneidner Jr., Phys. Rev. B **72**, 024416 (2005).

[48] A. O. Pecharsky, K. A. Gschneidner, Jr., and V. K. Pecharsky, J. Appl. Phys. **93**, 4722 (2003).

[49] J. P. Perdew, Phys. Rev. B **33**, 8822 (1986); J. P. Perdew and Y. Wang, Phys. Rev. B **33**, R8800 (1986).

[50] P. Bagno, O. Jepsen and O. Gunnarsson, Phys. Rev. B **40**, R1997 (1989).

[51] D. Paudyal, T. Saha-Dasgupta and A. Mookerjee, J. Phys.: Condens. Matter **16**, 2317 (2004).

[52] V. K. Pecharsky, K. A. Gschneidner, Jr., in *Magnetism and Structure in Functional Materials*, edited by A. Planes, L. Manosa, and A. Saxena, Springer Series in Materials Science, Vol. 79 (Springer, Heidelberg, 2005).